Lawrence Berkeley National Laboratory

Title
Effect of the chlorine substitution position of the end-group on intermolecular interactions and photovoltaic performance of small molecule acceptors

Authors
Li, Xiaojun
Angunawela, Indunil
Chang, Yuan
et al.

Broader context

Recently the development of low bandgap small molecule acceptors (SMAs) have promoted power conversion efficiency of polymer solar cells (PSCs) to over 17%. However, the structure-property relationship is still a key issue and huge challenge in the molecular design of new-generation SMAs. Herein, three couples of SMAs isomers were synthesized, with chlorine substitution on different position of its terminal benzene ring, for investigating the structure-property relationship. We found that the chlorine substitution position has significant influence on the physicochemical properties, molecular ordering and photovoltaic performance of the SMAs. Molecular packing behavior of the SMAs is tightly related to and determined by the configuration of their terminal groups, no matter what central fused ring of the SMAs. The results provide a direct insight to explore the structure-property relationship of the photovoltaic materials, thus to further guide the design of the SMAs. In addition, the abundant and stereoscopic π-π intermolecular interaction in the SMAs play an important role in promoting the molecules to form suitable packing and charge transporting channels. Thus, an appropriate design of SMAs with more diverse molecular interaction may be beneficial to improving the molecular order, forming suitable morphology in blend films, finally improving the efficiency of the PSCs.

Effect of Chlorine Substitution Position of End-group on Intermolecular Interaction and Photovoltaic Performance of Small Molecule Acceptors

Xiaojun Li,[a b c g] Indunil Angunawela,[d] Yuan Chang,[b g] Jiadong Zhou,[e] He Huang,[c] Lian Zhong,[c] Alex Liebman-Pelaez,[f] Chenhui Zhu,[f] Lei Meng,[a] Zengqi Xie,[e]* Harald Ade,[d]* He Yan,[b g] * Yongfang Li [a c h]*

[a] Beijing National Laboratory for Molecular Sciences, CAS Key Laboratory of Organic Solids, Institute of Chemistry, Chinese Academy of Sciences, Beijing 100190, China;

[b] Department of Chemistry and Hong Kong Branch of Chinese National Engineering Research Center for Tissue Restoration & Reconstruction,Hong Kong University of Science and Technology (HKUST), Clear Water Bay, Kowloon, Hong Kong, China;

[c] School of Chemical Science, University of Chinese Academy of Sciences, Beijing 100049, China;

[d] Department of Physics and Organic and Carbon Electronics Laboratories (ORaCEL), North Carolina State University, Raleigh, North Carolina 27695, USA;

[e] Institute of Polymer Optoelectronic Materials and Devices, State Key Laboratory of Luminescent Materials and Devices, South China University of Technology, Guangzhou 510640, China;

[f] Advanced Light Source, Lawrence Berkeley National Laboratory, Berkeley, California 94720, USA;

[g] Hong Kong University of Science and Technology-Shenzhen Research Institute, Shenzhen 518057, China;

[h] Laboratory of Advanced Optoelectronic Materials, College of Chemistry, Chemical Engineering and Materials Science, Soochow University, Suzhou, Jiangsu 215123, China.

E-mail: msxiez@scut.edu.cn (Z.X.), hwade@ncsu.edu (H.A.), hyan@ust.hk (H.Y.), liyf@iccas.ac.cn (Y.L.).

Abstract

The structure-property relationship of small molecular acceptors (SMAs) is a key issue in the molecular design of new-generation acceptor materials for further improving the device efficiencies of polymer solar cells (PSCs). Herein, three couples of SMAs isomers were synthesized, based on three central fused ring units and two IC isomer electron-withdrawing terminal units with chlorine substitution on different position of its benzene ring: Cl-1 with chlorine at the same side with C=O group of IC and Cl-2 with chlorine at the same side with CN groups of IC. Through systematical investigation, we found that the chlorine substitution position of the terminal groups has regular and significant influence on the molecular packing and photovoltaic performance of the SMAs. Molecular packing behavior of the SMAs is tightly related to and determined by the configuration of their terminal groups, no matter what central fused ring of the SMAs. Specifically, the Cl-1-based SMAs possess stronger crystallinity with long range ordering packing in its molecular plane direction, while the more abundant and stereoscopic π-π intermolecular interaction in the Cl-2-based SMAs promotes the molecules to form three-dimensional charge transporting channels and leads to their red-shifted absorption and higher electron mobilities. Therefore, the Cl-2-based PSCs exhibit higher power conversion efficiency (PCE) than that of the Cl-1-based devices, and the best PCE of a Cl-2 SMA-based PSC reached 16.42%. These results highlight the importance of the investigation of intermolecular interaction, packing and arrangement of the SMAs in the solid-state, which may provide a direct insight to explore the relationship between molecular structure and property of the photovoltaic materials. Moreover, we envision that if fragments like end group or side chains with more diverse molecular interaction are added in the design and synthesis of the SMAs, it may be beneficial to promoting the molecular π-π accumulation and further improving the molecular order, forming suitable molecular packing and morphology in blend films, finally affecting the efficiency of the PSCs.

Keywords: polymer solar cells, small molecule acceptors, intermolecular interaction, structure-property relationship, photovoltaic performance

Introduction

Polymer solar cells (PSCs) is a promising lightweight technology to utilizing low-cost renewable solar energy. [1-2] Under the considerable progress in materials and device processing methods, the power conversion efficiency (PCE) of single-junction PSCs has exceeded 16%.[3-10] The breakthrough of the PCE values in recent years is greatly attributed to the development of the acceptor-donor-acceptor (A-D-A) and A-DA'D-A-structured small molecule acceptors (SMAs).[11-16] This kind of SMAs, all exhibit highly anisotropic conjugated structures, which will affect their intermolecular interactions and lead to significant structure-property dependence.[17] The molecular packing plays a crucial role in determining intermolecular interactions, and the electronic and optical properties of the SMAs.[18] Moreover, the nanoscale ordering of the SMAs in solid state crucially affect mesoscale morphology of their blend films with polymer donors, and further influence the electron mobility, charge separation and charge collection ability of the PSCs.[19-20] Therefore, it is essential to study and understand the effect of the molecular structure on the intermolecular interactions and packing of the SMAs.

In recent years, many groups have performed a lot of research on the modification of the SMAs.[21-29] However, the relationships between structure, molecular packing and morphology of the blend films are still vague. Thus some researchers try to elucidate the structure-properties relationship of the SMAs through molecular structure modification. For instance, Marks and co-workers reported the SMAs of ITN-C9 and ITzN-C9, the difference between them is that the benzene substituents are located in different positions of terminal group. The divergent PCE outcomes of these molecules are associated with PCE-favorable "π-face-on" molecular orientation and increased crystallinity, which attributed to the difference of molecular structures.[30] Wei and co-workers carried out a calculation for explaining the importance of molecular arrangements on tuning the exciton binding energies of the SMAs.[31] Our group investigated the effects of side chain regiochemistry on the intermolecular interactions and aggregation behavior of the SMAs TPTC and TPTIC, and found significant effect of the side chain regiochemistry on the active layer morphology of the PSCs.[19] In addition, based on a series of SMAs, we also

illuminated the influence of the side chain length on the single-crystal packing of the SMAs, and on the photovoltaic performance of PSCs.[32] Morse and co-workers also emphasize the importance of side chain in molecular packing, and pointed out that the molecular fragments like electron deficient groups or side chains lead to a wide variety of geometrical conformations and adapt to facilitate molecular organization of the SMAs.[18] These studies indicate the importance of the fine structure modification on tuning the molecular packing and intermolecular interaction of the SMAs for understanding the structure-properties relationship.

In this work, we perform a systematic study on the structure-properties relationship of the SMAs by preparing three couples of SMA isomers with different chlorine substitution position on their terminal units (Fig.1), trying to explore how the chemical design can regularly influence the molecular organization of the SMAs and the device performance of the PSCs. The three couples of the SMA isomers are based on the central fused ring of MO-IDIC [33] (MO-IDIC-Cl-1 and MO-IDIC-Cl-2), fused ring of Y6 [6] (LY-Cl-1 and LY-Cl-2) and its derivative with longer side chains (N3-Cl-1 and N3-Cl-2) respectively, and chlorine substitution at different position of IC terminal groups: Cl-1 with chlorine at the same side with C=O group of IC and Cl-2 with chlorine at the same side with CN groups of IC (see Fig. 1a). The selection and design of the molecular structures are based on the following considerations: (1) The central fused rings are selected from the most representative SMAs including the most representative A-D-A-structured MO-IDIC and the A-DA'D-A-structured star molecule Y6. In addition, the different molecular shape of the two SMAs was also considered in the molecular design. (2) The common electron deficient terminal group (A unit) IC group [25] is selected as the terminal group of the SMAs. (3) Chlorination substitution at different positions of IC was designed for investigating the effect of the subtle chlorine substitution position on the intermolecular interactions and photovoltaic performance of the SMAs.

The absorption spectra, electronic energy levels, crystallinity, crystal packings, mesoscale morphology of the SMAs and their blend films with polymer donor, as well as the photovoltaic performance of the PSCs based on the three couples of SMA isomers are systematically studied and compared. We find that the chlorine substitution position

on the terminal group has the regular effect on the intermolecular interactions and photovoltaic performance of the three couples of SMAs no matter what central unit of them. The Cl-2-based SMAs exhibit red-shifted absorption spectra, down-shifted lowest unoccupied molecular orbital energy level (E_{LUMO}), higher degree of self-organization, more abundant intermolecular interaction and higher electron mobility than the Cl-1-based ones. In addition, the abundant molecular interaction of the Cl-2-based molecules should be the essential reason for its more ordered molecular stacking structure in the films. Photovoltaic properties of the three couples of SMAs are investigated by using PTQ10 [34], PM6 [35] and PL1 [36] as polymer donor respectively. The Cl-2-based SMAs all exhibit higher PCEs than that of its corresponding Cl-1-based molecules in the same couple of SMA isomers, which is mainly attributed to the improved FF due to the more ordered molecular accumulation and increased electron mobility of the Cl-2-based SMAs. The best PCE of the PSCs based on PL1:N3-Cl-2 reached 16.42%. These results demonstrate that the molecular packing is mainly predominated by structure fragment interactions, and molecular packing mode further plays a key role for the photovoltaic performance of the SMAs. Thus, the systematic study of molecular packing and refined structure design is effective in developing novel acceptor materials for achieving high photovoltaic efficiency.

Results and discussion

Synthesis of the SMAs

Molecular structures of the three fused ring monomers and the three series of isomeric acceptors based on them are shown in Fig. 1a. IC-Cl was synthesized according to the reported literature.[13] The two IC-Cl isomer units of Cl-1 and Cl-2 with chlorine substitution on different position of the benzene ring of the IC end group were successfully separated by column chromatography, the ^{1}H NMR and ^{13}C NMR spectra of these two end groups are shown in Figs. S10-S13. The final SMAs, MO-IDIC-Cl-1, MO-IDIC-Cl-2, LY-Cl-1, LY-Cl-2, N3-Cl-1 and N3-Cl-2 were synthesized by Knoevenagel condensation reactions between MO-IDT-CHO, LY-CHO, N3-CHO and Cl-1 and Cl-2, respectively. The detailed synthesis processes and purification details

are provided in Electronic Supporting Information (ESI†). The structure and purity

of the compounds were measured and confirmed by ^{1}H NMR, ^{13}C NMR spectra (Figs.
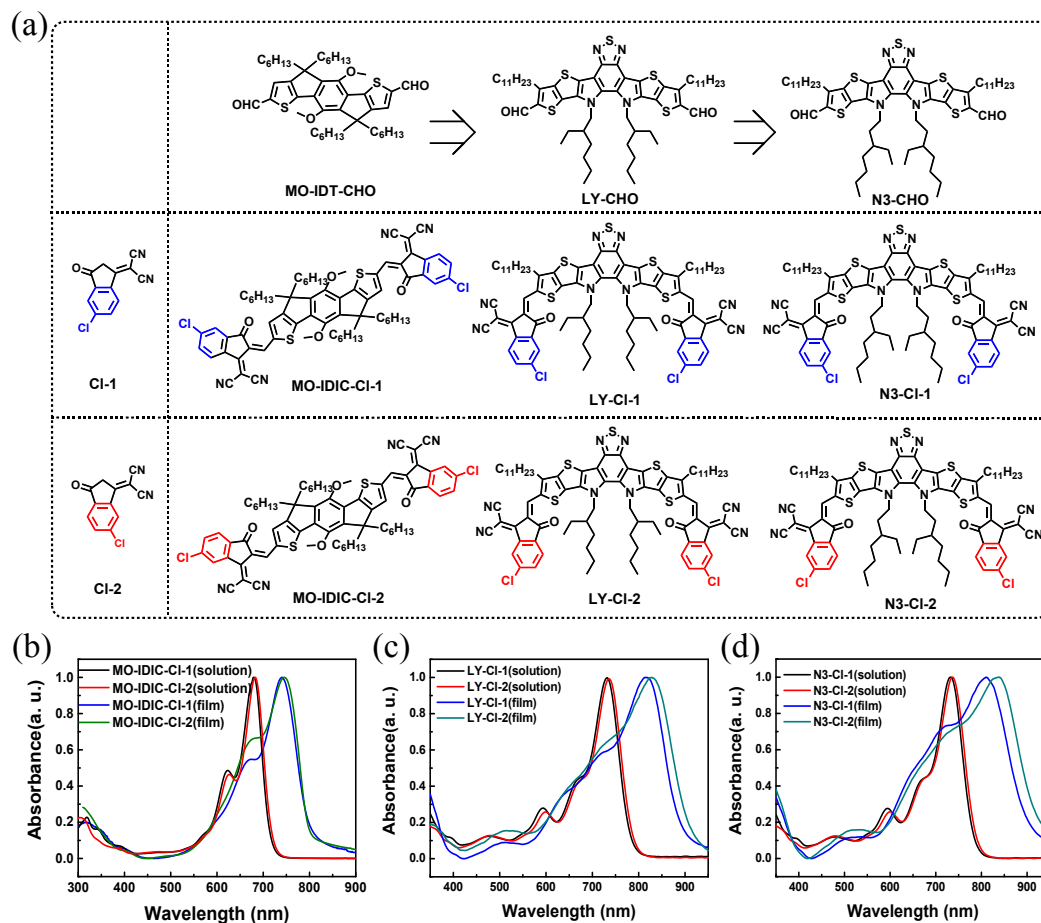
S14-S25) and mass spectroscopy.

Fig. 1 (a) Chemical structures of the three fused ring monomers, two isomers of end groups of Cl-1 and Cl-2, and the SMAs of MO-IDIC-Cl-1, MO-IDIC-Cl-2, LY-Cl-1, LY-Cl-2, N3-Cl-1and N3-Cl-2. Absorption spectra of (b) MO-IDIC-Cl-1 and MO-IDIC-Cl-2, (c) LY-Cl-1 and LY-Cl-2, (d) N3-Cl-1 and N3-Cl-2 in chloroform solutions and films state.

Absorption spectra and electronic energy levels

UV-vis absorption spectra (Figs. 1b-d) of the three series of SMAs in solution and

thin-film states were measured to investigate the effect of the chlorine substitution

position on the optical and aggregation properties of the acceptors. The corresponding

data are summarized in Table S1. In solutions, the acceptors with Cl-1 and Cl-2 terminal

groups exhibit similar absorption range from 550 to 730 nm for MO-IDIC-Cl-1 and MO-

IDIC-Cl-2, and from 550 to 800 nm for LY-Cl-1, LY-Cl-2, N3-Cl-1 and N3-Cl-2. Moreover, the Cl-2-based molecules (the acceptors with Cl-2 terminal groups) show slightly red-shifted absorption than the Cl-1-based ones. In films, all the SMAs exhibit red-shifted absorption in comparison with their solutions, which could be attributed to their ordered aggregation in films. In addition, the absorption spectra of the Cl-2-based SMAs show more obviously red-shifted absorption than that of the Cl-1-based ones in the films. This result indicates that the SMAs with Cl-2 terminal groups possess more ordered molecular packing, which will be beneficial to the more efficient charge transport in the PSCs.

The maximum absorption (λ_{max}) of these SMAs are at 740 nm, 746 nm, 816 nm, 829 nm, 811 nm and 838 nm, with optical band gaps (E_g^{opt}) of 1.55 eV, 1.54 eV, 1.39 eV, 1.36 eV, 1.37 eV and 1.33 eV for MO-IDIC-Cl-1, MO-IDIC-Cl-2, LY-Cl-1, LY-Cl-2, N3-Cl-1 and N3-Cl-2, respectively. Electronic energy levels of these SMAs were measured by electrochemical cyclic voltammetry, as shown in Fig. S3 and Table S1. The Cl-2-based SMAs exhibit slightly up-shifted the highest occupied molecular orbital (HOMO) energy level (E_{HOMO}), and down-shifted the lowest unoccupied molecular orbital (LUMO) energy level (E_{LUMO}) than the Cl-1-based SMAs. The E_{LUMO} and E_{HOMO} changing tendency of the Cl-2-based SMAs agrees with their red-shifted absorption and reduced E_g in comparison with the Cl-1-based SMAs, which may be attributed to the changes of dipole moment or electron cloud distribution in the molecules with the chlorine substitution on different position.[37]

Crystallinity and molecular packing of SMAs

For further investigating the effect of the chlorine substitution position on the aggregation of the SMAs, differential scanning calorimetry (DSC) was utilized to compare the thermal properties of the SMAs, as shown in Fig. 2. In the first heating of the DSC measurement, MO-IDIC-Cl-2 display obvious cold crystallization peak, with an enthalpy of 10.2 J/g but there is no clear melting peak. However, MO-IDIC-Cl-1 shows DSC melting peaks in both 1st and 2nd heating cycle, which are not shown in MO-IDIC-Cl-2, indicating that MO-IDIC-Cl-1 can crystalize from the melt, whereas MO-

Energy & Environmental Science

IDIC-Cl-2 needs the assistance of the solvent. This is likely related to different interactions between the end groups. As shown in Fig. 2 (b, e), LY-Cl-2 does not show any crystallization or melting peak, while LY-Cl-1 still shows a cold crystallization peak in the 1st heat with an enthalpy of 2.8 J/g, which means LY-Cl-1 is a little more crystalline than LY-Cl-2. Finally, comparing N3-Cl-1 and N3-Cl-2 (Fig. 2c, f), N3-Cl-1 shows two distinct peaks with enthalpies of 1.4 J/g and 3.5 J/g respectively, however N3-Cl-2 is mostly amorphous without any crystallizations or melting peaks. The results demonstrate the Cl-1-based molecule (N3-Cl-1) is more crystalline than N3-Cl-2. Collectively, it is interesting to note from the data above that, the SMAs with Cl-1 terminal groups exhibit higher degrees of crystallites than the Cl-2-based SMAs.
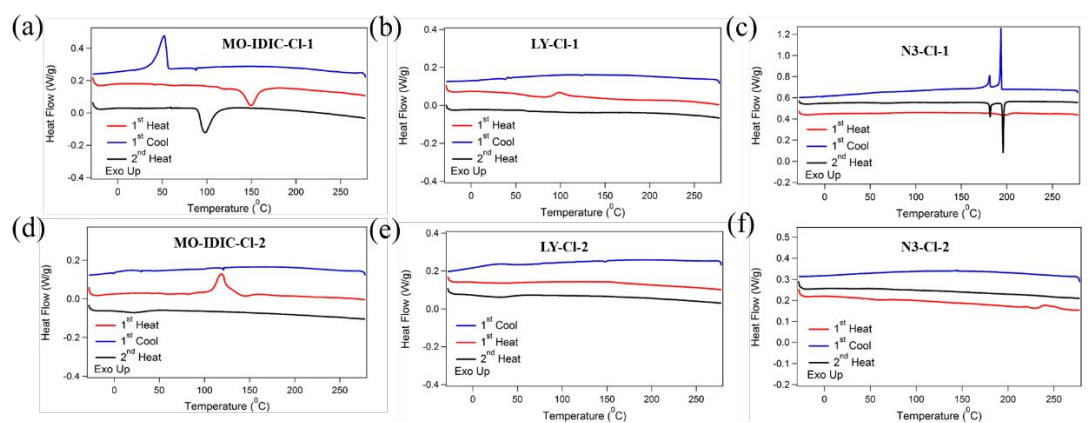

Fig. 2 DSC plots of (a) MO-IDIC-Cl-1, (b) LY-Cl-1, (c) N3-Cl-1, (d) MO-IDIC-Cl-2, (e) LY-Cl-2, (f) N3-Cl-2.

GIWAXS was further used to investigate the orientation, molecular packing and the crystallinity of the polymer donors of PTQ10, PM6 and PL1 (which will be used in fabrication of the PSCs to investigate the photovoltaic performance of the SMAs) and the six SMAs in neat films. We prepared these thin films on Si substrates by spin-coating from their chloroform solutions. The rapid evaporation of the solvent chloroform could quench the films in some disordered state due to different ability and kinetics of ordering aggregation of the photovoltaic materials. Fig. S4 displays 2D GIWAXS patterns of the polymer donors, which all show predominantly face-on orientation.
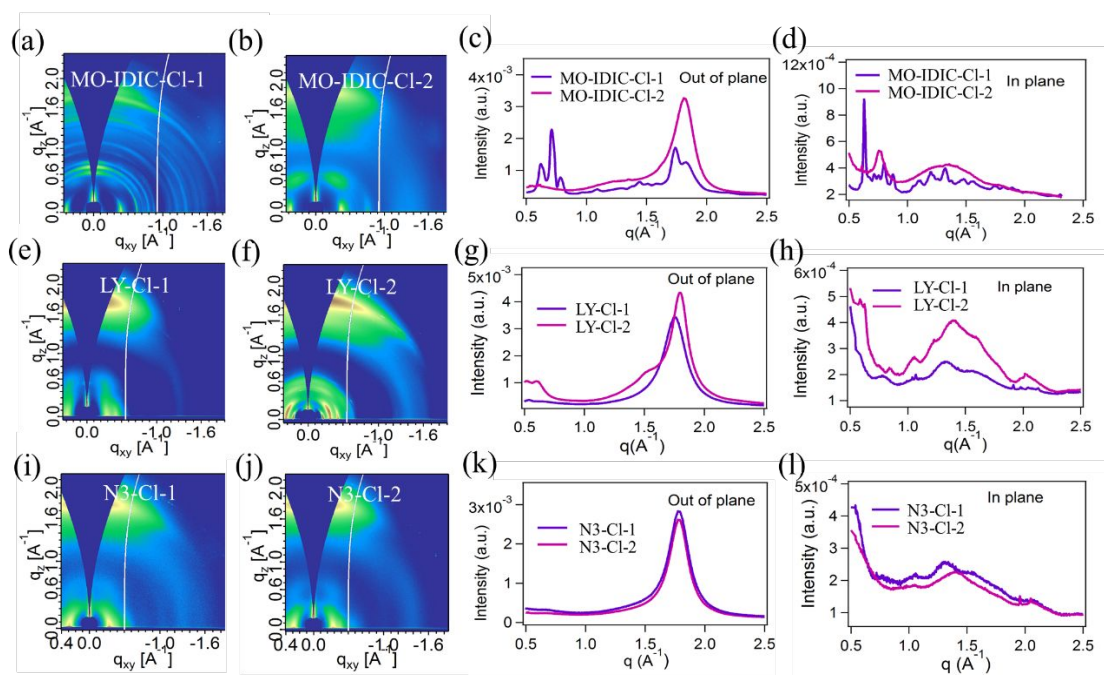
Fig. 3 2D GIWAXS patterns of (a) MO-IDIC-Cl-1, (b) MO-IDIC-Cl-2, (e) LY-Cl-1, (f) LY-Cl-2, (i) N3-Cl-1 and (j) N3-Cl-2 film; Line cuts of the GIWAXS of (c) MO-IDIC-Cl-1 and MO-IDIC-Cl-2, (g) LY-Cl-1 and LY-Cl-2, (k)N3-Cl-1 and N3-Cl-2 films in out-of-plane direction and (d) MO-IDIC-Cl-1 and MO-IDIC-Cl-2, (h) LY-Cl-1 and LY-Cl-2, (l)N3-Cl-1 and N3-Cl-2 films in in-plane direction.

Fig. 3 shows the 2D GIWAXS patterns of the SMAs neat films and their line cuts in the in-plane and out-of-plane directions. MO-IDIC-Cl-1 and MO-IDIC-Cl-2 exhibit predominantly face-on orientation with π-π stacking in the out-of-plane direction at about 1.83 $Å^{-1}$ (Fig. 3c), the π-π stacking distances and the coherence lengths of MO-IDIC-Cl-1 and MO-IDIC-Cl-2 films are similar, with a distance of 3.43 and 3.45 Å, and corresponding π-π stacking coherence lengths (CCL) of 48 and 46 Å, respectively. Compared with MO-IDIC-Cl-2, more scattering peaks are observed for MO-IDIC-Cl-1, suggesting that MO-IDIC-Cl-1 may adopt several different packing motifs or polymorphs and possesses higher degrees of aggregation than MO-IDIC-Cl-2. For the isomers of LY-Cl-1 and LY-Cl-2 (Fig. 3g, h), the π-π stacking diffraction is at 1.73 $Å^{-1}$ for LY-Cl-1 compared to 1.77 $Å^{-1}$ for LY-Cl-2 in the out-of-plane direction. The π-π stacking distance/CCL of these molecules are 3.63/16 Å for LY-Cl-1 and 3.55/18 Å for LY-Cl-2, which exhibits better π-π stacking and similar π-π stacking coherence length

of LY-Cl-2 compared to LY-Cl-1. The normalized integrated intensity of the π-π staking is higher in the Cl-2-based than the Cl-1-based MO-IDIC and LY SMAs, which indicates that the Cl-2-based SMAs possesses a higher degree of molecular packing than that of Cl-1 based ones in the spin-cast films. Both N3-Cl-1 and N3-Cl-2 SMAs pair show similar π-π staking distance (3.53 Å) and π-π stacking coherence length (33 Å for N3-Cl-1 and 35 Å for N3-Cl-2). However, the thickness normalized integrated intensity of the π-π staking is slightly higher in N3-Cl-2 than N3-Cl-1, which indicates the improved molecular order in the N3-Cl-2 film than the N3-Cl-1 film. In general, the results of GIWAXS reveal a noticeable common influence of the chlorine substitution position on the molecular packing: the Cl-2-based SMAs exhibit higher degree of self-organization and more ordered molecular packing in the π-π stacking direction than that of the Cl-1-based ones. This result is consistent with the conclusion obtained from the absorption spectra mentioned above.

Single crystals of the SMAs are free of grain boundaries and have long-range periodic order.[17] Hence, crystals structure of the SMAs could provide powerful information for examining the intermolecular interactions and structure-property relationships,[18, 38] which in turn further guides molecular design and syntheses. Thus, in order to explore the changes of molecular interaction and the difference of the ordered packing mode caused by the different position of chlorine substitution in the terminal group. The single-crystals of chlorinated terminal units Cl-1, Cl-2 and the SMAs were grown via slow diffusion of the poor solvent (methanol) to its good solvent (chloroform) solutions, then the corresponding diffraction data were acquired. The single-crystal structures of Cl-1 and Cl-2 are shown in Fig. 4a, b, which also exhibits the intermolecular interactions (broken line) between a central molecule (blue one) and adjacent ones. From this figure, Cl-1 and Cl-2 exhibit completely different packing motives, the interaction between Cl-1 and its adjacent molecules mostly tend to be extended in a plane, while the accumulation of Cl-2 is more stereoscopically extended. The different packing mode of the terminal units could affect the packing of the SMAs.

The configurations of MO-IDIC-Cl-1, MO-IDIC-Cl-2, LY-Cl-1 and LY-Cl-2 from their crystal structures are shown in Fig. S5, and the corresponding crystal data are listed

in Table S3. From the crystal structures, all the SMAs exhibit the intramolecular S···O=C interaction and especially additional S···O interaction for MO-IDIC, which may provide an interlocking structure to fix the molecular conformation. Chlorine atoms in these systems exhibit abundant interactions with adjacent molecules, including hydrogen bonding with side chains and weak interactions with CN groups, which play an important role in promoting molecular accumulation. In order to reveal the molecular interaction between the adjacent molecules for the SMAs, the in-pane molecules are marked as blue as references and the neighboring molecules with molecular interactions with reference one (central molecule) are shown in Figs. 4a, d, g, j, and owing to the side chains of the isomeric SMAs are the same, so alkyl chains are omitted for clarity. As shown in Fig. 4a, the central MO-IDIC-Cl-1 exhibits multiple intermolecular hydrogen bonding (Fig. S6) with CN···H distance of 2.45/2.51 Å between adjacent ICs and 2.81 Å between adjacent IC and MO-IDIC perpendicularly to the molecular long axis direction in plane. Furthermore, these molecules are extended by head-to-tail π-π stacking with average distance of 3.68 Å, and finally forms parallel arrangement (Fig. 4b, c). For MO-IDIC-Cl-2, there are two independent conformational molecules and three kinds of π-π interactions with average distance of 3.45 Å (Fig. 4d), which allows these molecules to form such cross-aligned network structure, and further promotes the layers of the large network to form a three-dimensional interpenetrating network structures (Fig. 4e).

As shown in Fig. 4g, LY-Cl-1 shows planar but not mirrored conformation, and the stacking pattern contains three kinds of π-π interactions with average distance of 3.59 Å and multiple hydrogen bonding (Fig. S6) with CN···H distances of 2.41 and 2.69 Å. The CN···H interactions lead to the molecules forming wave line extension in planar layer, and molecular layer stacked by multiple head-to-tail π-π interaction and steric effect of the side chains. Interestingly, more intermolecular interactions are found for the stacking structure of LY-Cl-2 than that of LY-Cl-1. In detail, as shown in Fig. 4j, head-to-tail, head-to-head (tail-to-tail) and core-to-core π-π stacking with average distance of 3.44 Å and hydrogen boding with S···H distance of 2.84 Å and N···H distance of 2.75 Å are cooperatively forming a complex three-dimensional framework in the LY-Cl-2 crystal (Fig. 4k).
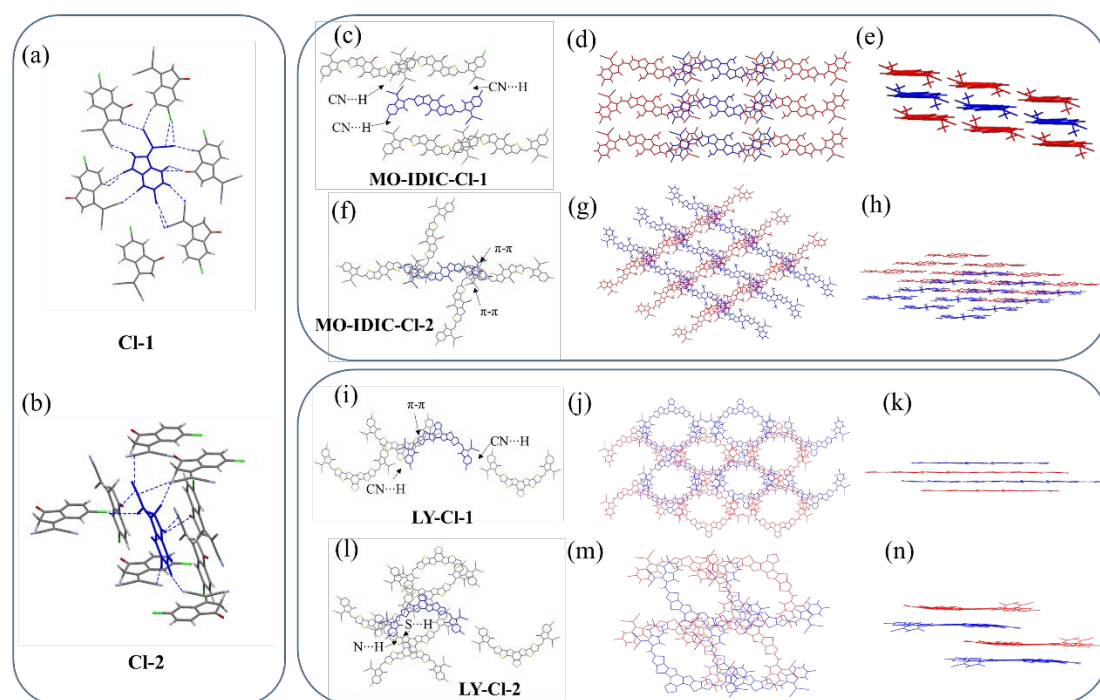
Fig. 4 Molecular configurations between the reference molecule and its neighboring molecules of (a) Cl-1, (b) Cl-2, (c)MO-IDIC-Cl-1, (f) MO-IDIC-Cl-2, (i) LY-Cl-1, (l) LY-Cl-2; Molecular stacking patterns of (d) MO-IDIC-Cl-1, (g) MO-IDIC-Cl-2, (j) LY-Cl-1, (m) LY-Cl-2 along their π plane; Molecular stacking patterns of (e) MO-IDIC-Cl-1, (h) MO-IDIC-Cl-2; (k)LY-Cl-1, (n)LY-Cl-2 perpendicular to their π plane.

Combining the accumulation of Cl-1 and Cl-2 to compare the interaction and packing mode between the Cl-1-based molecules and the Cl2-based ones, some interesting regular pattern caught our attention. Even though the MO-IDIC-Cl-1 (or Cl-2) and LY-Cl-1 (or Cl-2) have different molecular structures and shapes, their packing mode are still similar to that of the terminal electron pulling groups (Cl-1 and Cl-2). The intermolecular hydrogen-bonding connection between ICs is easier to form for the Cl-1 based compounds, which is conducive to their in-plane extension. However, interlinking hydrogen bonds are not conjugated and continuous in plane, which make scarce contributions for electron transport process. MO-IDIC-Cl-1 is packed into one-dimensional molecular aggregation mode, which limits the electron transporting channel. While for the Cl-2-based molecules, the intermolecular interactions are more abundant

and stereoscopic like Cl-2, which make molecular packing expanding in three-dimensional space. Moreover, the high dimensionality of the co-facial π-π stacking in the Cl-2-based molecules will provide efficient electronic coupling for charge transfer. Such as that MO-IDIC-Cl-2 forms a three-dimensional grid like accumulation, LY-Cl-2 forms a spatial network structure with obvious interlayer packing. These interpenetrating networks are beneficial for the rapid transfer of charge carriers along multiple directions.

The differences of the Cl-1 and Cl-2 based SMAs in crystallinity and molecular packing characteristics are likely due to the differences of their molecular packing during crystallization and film formation. For the Cl-1 based molecules with Cl-1 terminal groups, the multiple intermolecular hydrogen bonding could be conducive to their ordered extension in the direction of long range molecular plane but not in the π-π stacking direction, which leads the Cl-1 based molecules sowing stronger crystallinity than that of Cl-2 based molecules. While the abundant and stereoscopic π-π intermolecular interaction of the Cl-2 based SMAs lead to more ordered short-range stacking in the π-π direction, as observed in the GIWAXS measurement, which is beneficial to the charge transfer in the Cl-2 based SMAs. Table S2 in ESI lists the electron mobilities of the SMAs measured by space charge limited current (SCLC) method. The electron mobilities of the Cl-2-based SMAs are obviously higher than those of the Cl-1-based SMAs (7.31×10^{-4} for MO-IDIC-Cl-2 vs. 5.11×10^{-4} cm^2 V^{-1} s^{-1} for MO-IDIC-Cl-1, 7.08×10^{-4} for LY-Cl-2 vs. 4.56×10^{-4} cm^2 V^{-1} s^{-1} for LY-Cl-1, 14.8×10^{-4} for N3-Cl-2 vs. 5.75×10^{-4} cm^2 V^{-1} s^{-1} for N3-Cl-1), which consists with the molecular packing structures.

Photovoltaic performance

All these results of optical properties, electronic energy levels, crystallinity and electron mobilities show that the subtle difference of the structures have significant impacts on the molecular packing structure and properties of the SMAs. In order to systematically understand the influence of the position difference of terminal chlorine atoms on their photovoltaic performance, the PSCs with a conventional configuration of

ITO/PEDOT: PSS/ polymers: SMAs /PDINO/Al were fabricated, in which medium bandgap conjugated polymers PTQ10, PM6 and PL1 (see Fig. S2 in ESI) were used as the electron donors. The reason of selecting different polymers as donor is to form a better energy level matching between the acceptors and donors, and the slightly up-shifted HOMO level of PL1 compared with that of PM6 would be beneficial to match with the N3-Cl-1(or Cl-2) with upshifted HOMO energy levels compared with LY-Cl-1(or Cl-2).[36] PEDOT:PSS and PDINO served as the anode and cathode buffer layers, respectively. The devices using chloroform as processing solvent and the donor/acceptor (D:A) weight ratios in the blend active layers were optimized to 1:1.1 (*wt/wt*) for PTQ10:MO-IDIC-Cl-1(or 2) and PM6:LY-Cl-1(or 2) systems with thermal annealing at 110 °C for 5 min. The optimized D:A weight ratio for PL1: N3-Cl-1(or 2) is 1:1.5 and the thermal annealing is at 100°C for 5 min. The current density-voltage (*J-V*) curves and incident photon to current conversion efficiency (IPCE) spectra of the PSCs for the three systems are shown in Fig. 5 and the detailed photovoltaic parameters are summarized in Table 1.
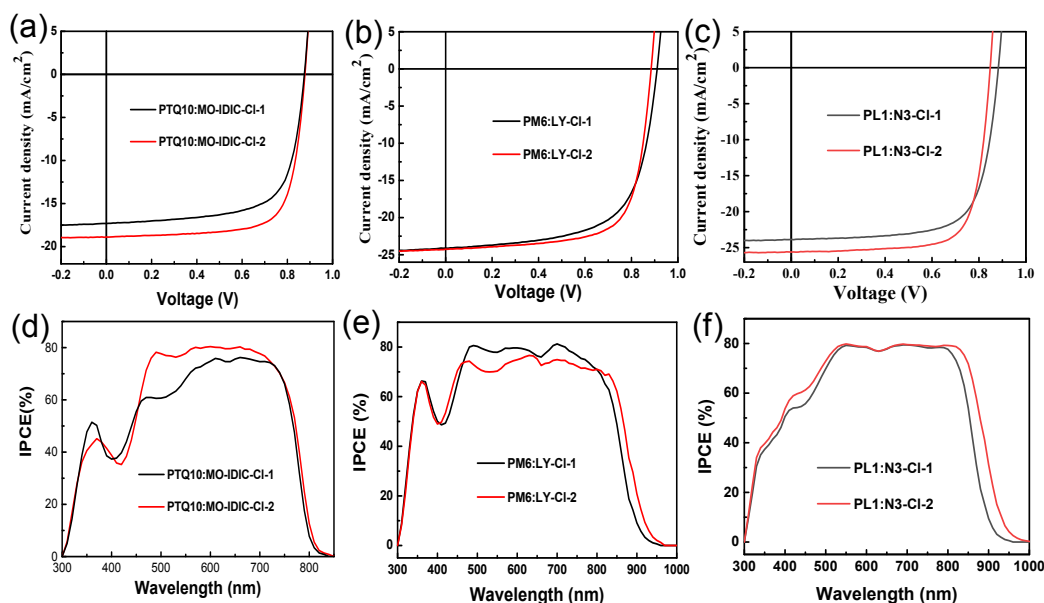

Fig. 5 *J-V* curves of the optimized PSCs based on (a) PTQ10: MO-IDIC-Cl-1 or MO-IDIC-Cl-2, (b) PM6:LY-Cl-1 or LY-Cl-2, (c) PL1:N3-Cl-1 or N3-Cl-2 under the illumination of AM 1.5G, 100 mW cm^{-2}; IPCE spectra of the correcpong PSCs based on (d) PTQ10: MO-IDIC-Cl-1 or MO-IDIC-Cl-2, (e) PM6:LY-Cl-1 or LY-Cl-2, (f)

PL1:N3-Cl-1 or N3-Cl-2.

Table 1 Photovoltaic Performance Parameters of the PSCs Based on Corresponding Donors: Acceptors under the Illumination of AM1.5G, 100 mW cm^{-2}

Acceptor	Donor	V_{oc}	J_{sc}	FF	PCE[c]	J_{sc} from IPCE
		(V)	(mA cm^{-2})	（%）	(%)	(mA cm^{-2})
MO-IDIC-Cl-1[a]	PTQ10	0.88	17.67	69.2	10.76	17.16
MO-IDIC-Cl-2[a]		0.88	19.21	73.9	12.49	18.66
LY-Cl-1[a]	PM6	0.91	24.30	65.1	14.41	23.37
LY-Cl-2[a]		0.88	24.19	70.9	15.16	23.15
N3-Cl-1[b]	PL1	0.88	23.86	71.4	15.05	23.04
N3-Cl-2[b]		0.85	25.62	75.5	16.42	24.77

[a] With thermal annealing at 110 °C for 5 min. [b] With thermal annealing at 100 °C for 5 min. [c] Data are average values calculated from more than 20 devices.

For the PTQ10:MO-IDIC-Cl-1(or 2) system, the devises with MO-IDIC-Cl-1 as acceptor exhibit a PCE of 10.76%, with a V_{oc} of 0.88 V, J_{sc} of 17.67 mA cm^{-2}, and FF of 69.2%. The MO-IDIC-Cl-2 based PSCs show better photovoltaic performance with a PCE of 12.49%, the V_{oc}, J_{sc} and FF are 0.88 V, 19.21 mA cm^{-2} and 73.9% respectively. Among the LY-Cl-1 and LY-Cl-2 based devises, the PM6: LY-Cl-1 devices yield a PCE of 14.41%, with a V_{oc} of 0.91 V, J_{sc} of 24.30 mA cm^{-2}, and FF of 65.1%. The LY-Cl-2 based PSCs show a higher PCE of 15.16% with slightly lower V_{oc} of 0.88 V, similar J_{sc} of 24.19 mA cm^{-2}, but the higher FF of 70.9%, in coparison with that of the LY-Cl-1-based PSCs. For the PSCs with N3-Cl-1 or N3-Cl-2 as acceptor and PL1 as donor, the N3-Cl-1 based devices show a good PCE of 15.05% with V_{oc} of 0.88 V, J_{sc} of 23.86 mA cm^{-2}, and FF of 71.4%, while the N3-Cl-2-based PSCs display even higher PCE of 16.42% benefitted from simultaneously enhanced FF of 75.5% and J_{sc} of 25.62 mA cm^{-2} than that of the N3-Cl-1 based devices. The IPCE spectra (Figs. 5d-f) of these PSCs display a broadened photo-response, and the calculated J_{sc} values from the integration of the IPCE curves are listed in Table 1, which are in good agreement with those from *J-V*

measurements.

Comparing the photovoltaic parameters of the PSCs based the three couples of isomeric SMAs, there is noteworthy changing tendency: the Cl-2-based devices show higher PCE with slightly lower (or similar) V_{oc}, higher (or similar) J_{sc} ad higher FF than those of the Cl-1-based ones. The lower V_{oc} is due to the down-shifted LUMO level of the Cl-2-based SMAs, the higher J_{sc} values are benefited from the extended absorption the Cl-2-based SMAs. The increased PCEs of the Cl-2-based PSCs are mainly ascribed to their improved FF values, from MO-IDIC-Cl-1 (69.2%) to MO-IDIC-Cl-2 (73.9%), from LY-Cl-1 (65.1%) to LY-Cl-2 (70.9%) and from N3-Cl-1 (71.4%) to LY-Cl-2 (75.5%). The improved FF should be benefitted from the higher electron mobility of the Cl-2 SMAs (see Table S2). In addition, when using unseparated IC-Cl as the terminal group, the PCE of the corresponding acceptors are between the efficiency of the Cl-1-based and Cl-2-based SMAs (see Tables S4). These results indicate that the refined molecular structure design is an effective way in developing high efficiency photovoltaic materials.

Morphology analysis

In order to gain a deeper understanding about the relationship between the molecular structure of the SMAs and the device performance of their PSCs, we conducted GIWAXS measurements[39] on the blend films based on the three couples of isomeric SMAs. As shown in Fig. 6, all the blend films show predominantly face-on orientation. For the MO-IDIC-Cl-1 and MO-IDIC-Cl-2 based films, the corresponding π-π stacking distances of the SMAs in out-of-plane direction are the same (3.45 Å). However, the polymer donor π-π stacking distances are decreased (from 3.59 Å for the blend with MO-IDIC-Cl-1 to 3.51 Å for the blend with MO-IDIC-Cl-2), which suggests a closer packing of PTQ10 in the MO-IDIC-Cl-2 based blend film. In addition, significantly stronger and sharper π-π stacking peaks are observed in the PTQ10: MO-IDIC-Cl-2 film, and longer coherence length of the SMA in PTQ10: MO-IDIC-Cl-2 (47 Å) than that in MO-IDIC-Cl-1 (36 Å) based film are obtained, which is beneficial for charge transport in the vertical direction. In the GIWAXS pattern of PM6:LY-Cl-1 and

PM6:LY-Cl-2 blend films, it is not possible to deconvolve the contribution of the SMA and polymer donor for π-π stacking (Fig. 6g and Fig. 6h). The π-π stacking distance of 3.61 Å for both the blends and the coherence length of 32 Å and 33 Å respectively for the LY-Cl-1 and LY-Cl-2 based blend films does not show much difference. However, the thickness normalized integrated intensity of the out-of-plane π-π peak in the LY-Cl-2 blends is higher than the LY-Cl-1 blends, which should be attributed mostly from the improved ordering of LY-Cl-2. Fig. 6k and 6i show the results of PL1:N3-Cl-1 and PL1:N3-Cl-2 blend films. From the measurements, the similar SMA π-π stacking distance (3.55 Å for N3-Cl-1 and 3.57 Å for N3-Cl-2) and the coherence length (49 Å for N3-Cl-1 and 47 Å for N3-Cl-2) are obtained in these two blend films for SMAs. Similarly, the polymer π-π stacking distance (3.63 Å for N3-Cl-1-based blend and 3.61 Å for N3-Cl-2-based blend) and the coherence length (19 Å for N3-Cl-1-based blend and 20 Å for N3-Cl-2-based blend) does not show significant difference. Nonetheless, the intensity of the out-of-plane direction clearly increased in the N3-Cl-2 based films than the PL1:N3-Cl-1 blends, which should be attributed mostly from the improved ordering of the N3-Cl-2 acceptor. Summarizing these three systems, the packing difference caused by molecular interaction in the SMAs not only affects the properties of their neat films, but also influence the corresponding properties of their blend films with polymer donors, and this may be due to the distinctive packing mode of SMAs in the single crystal are most likely still preserve in the films.[40] The surface morphology of corresponding blend films was studied by atomic force microscopy (AFM). As shown in Fig. S7, there is no obvious difference between the Cl-1-based and Cl-2-based films. Therefore, the surface morphology has little effect on the properties of the blend films. Finally, the improved molecular ordering and the molecular aggregation of the Cl-2 based SMAs in the blend films are beneficial for the improvement of electron mobilities and therefore result in higher photovoltaic efficiencies for the PSCs with the Cl-2-based SMAs as acceptors.
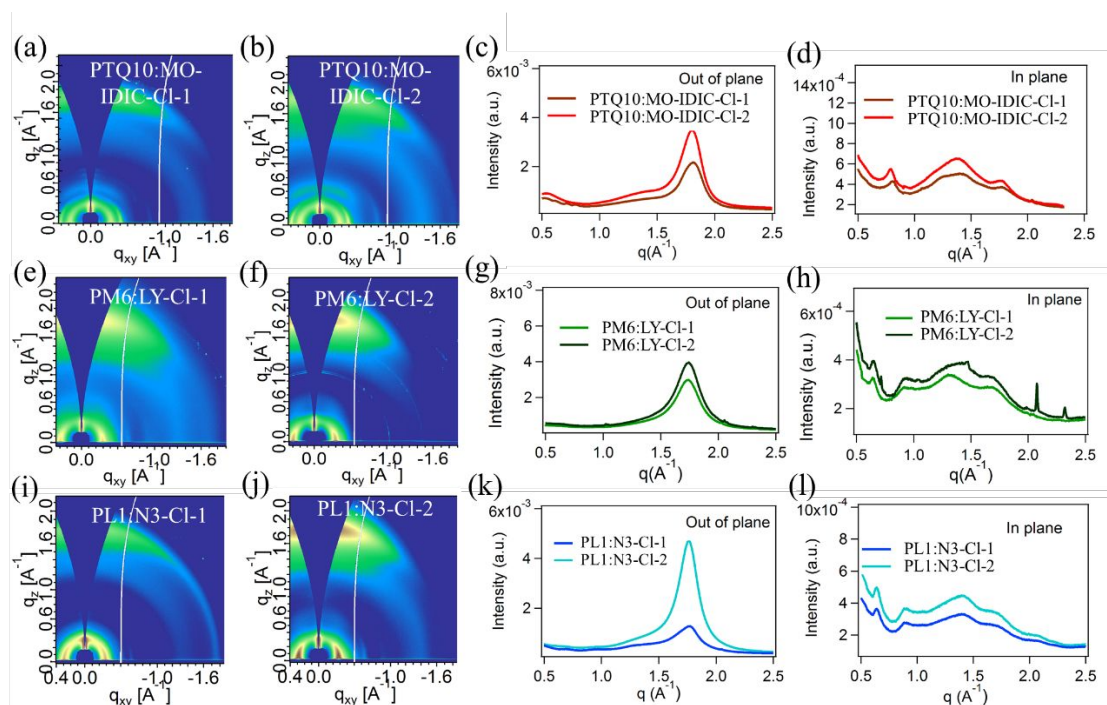
Fig. 6 2D GIWAXS patterns of the blend films of (a) PTQ10: MO-IDIC-Cl-1, (b) PTQ10: MO-IDIC-Cl-2, (e) PM6:LY-Cl-1, (f) PM6:LY-Cl-2, (i) PL1:N3-Cl-1 and (j) PL1:N3-Cl-2; Line cuts of GIWAXS of the blend films of (c) PTQ10: MO-IDIC-Cl-1 or MO-IDIC-Cl-2, (g) PM6:LY-Cl-1 or LY-Cl-2, (k) PL1:N3-Cl-1 or N3-Cl-2 in out of plane direction; Line cuts of GIWAXS of the blend films of (d) PTQ10: MO-IDIC-Cl-1 or MO-IDIC-Cl-2, (h) PM6:LY-Cl-1 or LY-Cl-2, (l) PL1:N3-Cl-1 or N3-Cl-2 in in-plane direction.

Conclusion

We have demonstrated that the small change in chlorine substitution position of the terminal IC electron deficient groups has significant influence on the properties and molecular ordering of the SMAs based on three different central fused ring units. A couple of new A-D-A SMAs with the same central fused ring of MO-IDIC (MO-IDIC-Cl-1 and MO-IDIC-Cl-2) and two couples of A-DA'D-A SMAs with the central units of Y6 (LY-Cl-1 and LY-Cl-2) and its derivative with longer side chains (N3-Cl-1 and N3-Cl-2) were synthesized by using chlorine substituted IC isomeric terminal groups: Cl-1 with chlorine at the same side with C=O group of IC and Cl-2 with chlorine at the same side with CN groups of IC. Detailed investigations of the molecular interaction are

carried out for understanding structure-property relationships in the three couples of SMAs isomers. It is found that there is regular influence of the chlorine substitution position of the terminal groups on the molecular interaction and photovoltaic performance of the SMAs. The Cl-2-based SMAs exhibit slightly red-shifted absorption, up-shifted E_{HOMO} and down-shifted E_{LUMO}, three-dimensional interpenetrating network structure with high ordered π-π direction molecular packing and significantly higher electron mobility than those of its corresponding Cl-1-based isomers. In comparison of the photovoltaic performance of the SMA isomers with the same central fused ring and different terminal groups of Cl-1 and Cl-2, the Cl-2 SMA-based PSCs show higher PCE with higher FF for all the three series of SMAs, and the best PCE of PSCs based on N3-Cl-2 reached 16.42%. Thus, an appropriate design of SMAs is important for the molecular aggregation and electron transporting network in the solid-state. Our results indicate that the introduction of suitable substituents at suitable position to promote intermolecular interaction should be an efficient way to improve the molecular stacking of the photovoltaic materials for further increasing PCE of the PSCs.

Conflicts of interest

There are no conflicts to declare.

Acknowledgements

Author Contributions

X.L. designed, synthesized and characterized the three couples of acceptors and the polymer donor of PL1, Y.C., H.H., L.Z. and L.M. performed the device fabrication and characterization of PSCs, X.L. J.Z. and Z.X. prepared the crystals and analyzed the crystal structure of acceptors, I.A., A.L.-P., C.Z. and H.A. measured and analyzed the GIWAXS results, Y.L. and H.Y. supervised the project, X.L, Z.X., H.A., H.Y. and Y.L. wrote the paper.

Notes and references

1   R. Søndergaard, M. Hösel, D. Angmo, T. T. Larsen-Olsen and F. C. Krebs, *Mater. Today*, 2012, **15**, 36-49.

2   C. J. Traverse, R. Pandey, M. C. Barr and R. R. Lunt, *Nat. Energy*, 2017, **2**, 849-860.

3   B. Fan, D. Zhang, M. Li, W. Zhong, Z. Zeng, L. Ying, F. Huang and Y. Cao, *Sci. China Chem.*, 2019, **62**, 746-752.

4   S. Liu, J. Yuan, W. Deng, M. Luo, Y. Xie, Q. Liang, Y. Zou, Z. He, H. Wu and Y. Cao, *Nat. Photonics*, 2020, **14**, 300-305.

5   Y. Cui, H. Yao, J. Zhang, T. Zhang, Y. Wang, L. Hong, K. Xian, B. Xu, S. Zhang, J. Peng, Z. Wei, F. Gao and J. Hou, *Nat. commun.*, 2019, **10**, 2515.

6   J. Yuan, Y. Zhang, L. Zhou, G. Zhang, H.-L. Yip, T.-K. Lau, X. Lu, C. Zhu, H. Peng, P. A. Johnson, M. Leclerc, Y. Cao, J. Ulanski, Y. Li and Y. Zou, *Joule*, 2019, **3**, 1140-1151

7   C. Sun, S. Qin, R. Wang, S. Chen, F. Pan, B. Qiu, Z. Shang, L. Meng, C. Zhang, M. Xiao, C. Yang and Y. Li, *J. Am. Chem. Soc.*, 2020, **142**, 1465-1474.

8   L. Zhu, M. Zhang, G. Zhou, T. Hao, J. Xu, J. Wang, C. Qiu, N. Prine, J. Ali, W. Feng, X. Gu, Z. Ma, Z. Tang, H. Zhu, L. Ying, Y. Zhang and F. Liu, *Adv. Energy Mater.*, 2020, **10**, 1904234.

9   Z. Zhou, W. Liu, G. Zhou, M. Zhang, D. Qian, J. Zhang, S. Chen, S. Xu, C. Yang, F. Gao, H. Zhu, F. Liu and X. Zhu, *Adv. Mater.*, 2020, **32**, 1906324.

10   K. Jiang, Q. Wei, J. Y. L. Lai, Z. Peng, H. K. Kim, J. Yuan, L. Ye, H. Ade, Y. Zou and H. Yan, *Joule*, 2019, **3**, 3020-3033.

11   L. Feng, J. Yuan, Z. Zhang, H. Peng, Z. G. Zhang, S. Xu, Y. Liu, Y. Li and Y. Zou, *ACS Appl. Mater. Interfaces*, 2017, **9**, 31985-31992.

12   Y. Lin, Q. He, F. Zhao, L. Huo, J. Mai, X. Lu, C. J. Su, T. Li, J. Wang, J. Zhu, Y. Sun, C.

Wang and X. Zhan, *J. Am. Chem. Soc.*, 2016, **138**, 2973-2976.

13   Y. Lin, J. Wang, Z. G. Zhang, H. Bai, Y. Li, D. Zhu and X. Zhan, *Adv. Mater.*, 2015, **27**, 1170-1174.

14   N. Qiu, H. Zhang, X. Wan, C. Li, X. Ke, H. Feng, B. Kan, H. Zhang, Q. Zhang, Y. Lu and Y. Chen, *Adv. Mater.*, 2017, **29**, 1604964.

15   W. Zhao, S. Li, H. Yao, S. Zhang, Y. Zhang, B. Yang and J. Hou, *J. Am. Chem. Soc.*, 2017, **139**, 7148-7151.

16   W. Gao, M. Zhang, T. Liu, R. Ming, Q. An, K. Wu, D. Xie, Z. Luo, C. Zhong, F. Liu, F. Zhang, H. Yan and C. Yang, *Adv. Mater.*, 2018, **30**, 1800052.

17   C. Wang, H. Dong, L. Jiang and W. Hu, *Chem. Soc. Rev.*, 2018, **47**, 422-500.

18   P. Mondelli, G. Boschetto, P. N. Horton, P. Tiwana, C.-K. Skylaris, S. J. Coles, M. Krompiec and G. Morse, *Mater. Horiz.*, 2020, **7**, 1062-1072.

19   X. Li, H. Huang, Z. Peng, C. Sun, D. Yang, J. Zhou, A. Liebman-Pelaez, C. Zhu, Z.-G. Zhang, Z. Zhang, Z. Xie, H. Ade and Y. Li, *J. Mater. Chem. A,* 2018, **6**, 15933-15941.

20   Z. Zhang, J. Yu, X. Yin, Z. Hu, Y. Jiang, J. Sun, J. Zhou, F. Zhang, T. P. Russell, F. Liu and W. Tang, *Adv. Funct. Mater.*, 2018, **28**, 1705095.

21   S. Li, L. Zhan, F. Liu, J. Ren, M. Shi, C. Z. Li, T. P. Russell and H. Chen, *Adv. Mater.*, 2018, **30**, 1705208.

22   J. Sun, X. Ma, Z. Zhang, J. Yu, J. Zhou, X. Yin, L. Yang, R. Geng, R. Zhu, F. Zhang and W. Tang, *Adv. Mater.*, 2018, **30**, 1707150.

23   Z. Yao, X. Liao, K. Gao, F. Lin, X. Xu, X. Shi, L. Zuo, F. Liu, Y. Chen and A. K. Jen, *J. Am. Chem. Soc.*, 2018, **140**, 2054-2057.

24   T. J. Aldrich, M. Matta, W. Zhu, S. M. Swick, C. L. Stern, G. C. Schatz, A. Facchetti, F. S. Melkonyan and T. J. Marks, *J. Am. Chem. Soc.*, 2019, **141**, 3274-3287.

25   H. Lai, H. Chen, J. Zhou, J. Qu, P. Chao, T. Liu, X. Chang, N. Zheng, Z. Xie and F. He, *iScience*, 2019, **17**, 302-314.

26   Y. Li, N. Zheng, L. Yu, S. Wen, C. Gao, M. Sun and R. Yang, *Adv. Mater.*, 2019, **31**, 1807832.

27   H. Lai, Q. Zhao, Z. Chen, H. Chen, P. Chao, Y. Zhu, Y. Lang, N. Zhen, D. Mo, Y. Zhang and F. He, *Joule*, 2020, **4**, 688-700.

28   Z. Fei, F. D. Eisner, X. Jiao, M. Azzouzi, J. A. Rohr, Y. Han, M. Shahid, A. S. R. Chesman, C. D. Easton, C. R. McNeill, T. D. Anthopoulos, J. Nelson and M. Heeney, *Adv. Mater.*, 2018. **30**, 1705209.

29   Z. Luo, H. Bin, T. Liu, Z. G. Zhang, Y. Yang, C. Zhong, B. Qiu, G. Li, W. Gao, D. Xie, K. Wu, Y. Sun, F. Liu, Y. Li and C. Yang, *Adv. Mater.*, 2018, **30**, 1706124.

30   S. M. Swick, W. Zhu, M. Matta, T. J. Aldrich, A. Harbuzaru, J. T. Lopez Navarrete, R. Ponce Ortiz, K. L. Kohlstedt, G. C. Schatz, A. Facchetti, F. S. Melkonyan and T. J. Marks, *Proc. Natl. Acad. Sci.*, 2018, **115**, E8341-E8348.

31   L. Zhu, Z. Tu, Y. Yi and Z. Wei, *J. Phys. Chem. Lett.*, 2019, **10**, 4888-4894.

32   X. Li, H. Huang, I. Angunawela, J. Zhou, J. Du, A. Liebman‐Pelaez, C. Zhu, Z. Zhang, L. Meng, Z. Xie, H. Ade and Y. Li, *Adv. Funct. Mater.*, 2020, **30**, 1906855.

33   X. Li, F. Pan, C. Sun, M. Zhang, Z. Wang, J. Du, J. Wang, M. Xiao, L. Xue, Z. G. Zhang, C. Zhang, F. Liu and Y. Li, *Nat. Commun.*, 2019, **10**, 519.

34   C. Sun, F. Pan, H. Bin, J. Zhang, L. Xue, B. Qiu, Z. Wei, Z. G. Zhang and Y. Li, *Nat.*

Commun., 2018, **9**, 743.

35   Q. Fan, W. Su, Y. Wang, B. Guo, Y. Jiang, X. Guo, F. Liu, T. P. Russell, M. Zhang and Y. Li, *Sci. China Chem.*, 2018, **61**, 531-537.

36   X. Li, R. Ma, T. Liu, Y. Xiao, G. Chai, X. Lu, H. Yan and Y. Li, *Sci. China Chem.*, 2020, **63**, DOI:10.1007/s11426-020-9805-7.

37   S. Li, L. Ye, W. Zhao, S. Zhang, H. Ade and J. Hou, *Adv. Energy Mater.*, 2017, **7**, 1700183.

38   M. Mas-Torrent and C. Rovira, *Chem. Rev.*, 2011, **111**, 4833-4856.

39   A. Hexemer, W. Bras, J. Glossinger, E. Schaible, E. Gann, R. Kirian, A. MacDowell, M. Church, B. Rude and H. Padmore, *J. Phys.: Conf. Ser.*, 2010, **247**, 012007.

40   G. Zhang, X. Chen, J. Xiao, P. Chow, M. Ren, G. Kupgan, X. Jiao, C. Chan, X. Du, R.Xia, Z. Chen, J. Yuan, Y. Zhang, S. Zhang, Y. Liu, Y. Zou, H. Yan, K. Wong, V. Coropceanu, N. Li, C. J. Brabec, J. -L. Bredas, H.-L. Yip and Y. Cao, *Nat. Commun.*, 2020, **11**, 3943.

Effect of Chlorine Substitution Position of End-group on Intermolecular Interaction and Photovoltaic Performance of Small Molecule Acceptors

Xiaojun Li, Indunil Angunawela, Yuan Chang, Jiadong Zhou, He Huang, Lian Zhong, Alex Liebman-Pelaez, Chenhui Zhu, Lei Meng, Zengqi Xie,* Harald Ade,* He Yan, * Yongfang Li *

Keywords: polymer solar cells, small molecule acceptors, intermolecular interaction, structure-property relationship, photovoltaic performance

TOC figure:
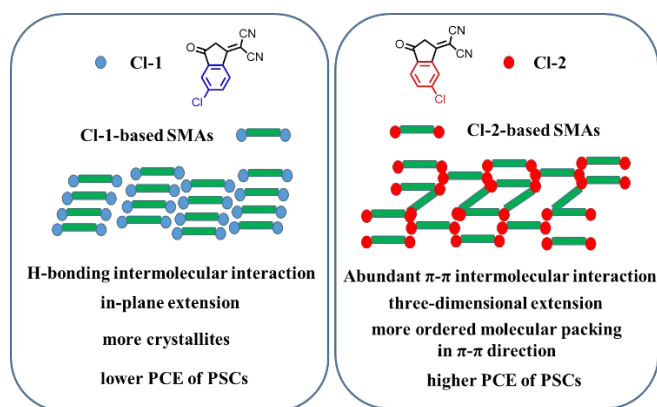
Difference in intermolecular interaction of small molecule acceptors with different chlorine substitution position affects their molecular packing and photovoltaic property